Improvement of alkali resistance of glass fiber from basalt and lignite bottom ash mixture by addition of ZrO₂ content

Apirat THEERAPAPVISETPONG[1,*], Phraethong KWANPANNGAM[1] and Thanapat TAMRONGWONGWIT[1]

[1] *Department of Materials Science, Faculty of Science, Chulalongkorn University, Bangkok, 10330, Thailand*

Corresponding author e-mail: apirat.t@chula.ac.th

Abstract

In this work, silica-rich basalt from Chai Badan, Lopburi province was melted with lignite bottom ash from Mae Moh power plant as fluxing agent. To improving the alkali resistance, the series of glass batch samples were varied amount of ZrO_2 content by 0 wt% to 10 wt%. The batches were melted at 1500°C and drawn into a fiber. The results found that the alkali resistance of basalt fiber sample increase with increasing of ZrO_2 content up to 7.5 wt% ZrO_2. The sample with 7.5 wt% ZrO_2 performed the highest alkali resistance, while the sample with 5 wt% ZrO_2 obtained the highest tensile strength. The alkali resistance of these basalt fibers was given by a formation of stable hydrated zirconium-rich layer retarding the preinitiation of OH⁻ inside the surface. The corrosion of shell thickness of higher ZrO_2 content fiber increased at a slower rate according to its higher alkali resistance. The excess addition of ZrO_2 content up to 10 wt% in glass composition resulted in an increase of brittleness and weakness of the fiber caused by a defect from undissolved ZrO_2 crystal in a fiber and its solubility limit.

1. Introduction

Nowadays, basalt fiber is become a high potential in many composite materials. Because of its good mechanical and chemical properties, it has been used in reinforcing various composite materials such as concrete, boat, wind turbine blade, automotive and sport goods [1]. It is made from volcanic rock that can directly be melted and drawn to a fiber at temperature between 1500°C to 1700°C [2,3]. Basalt rock is found in many locations all over Thailand. It was defined as an alkali basalt. Cenozoic volcanic rocks outcrop in the central portion of the Loei-Phetchabun volcanic belt in central Thailand in the Lopburi area. These volcanic rocks ranged in composition from basalt to high-silica rhyolite [4,5]. However, there are some of basalt compositions can be used as a raw material for fiber production. The major components of basalt are SiO_2, Al_2O_3, CaO, MgO, Fe_2O_3 and FeO [6]. The typical composition of basalt fiber is 43.3 wt% to 55.69 wt% SiO_2, 11 wt% to 17.97 wt% Al_2O_3, 7.43 wt% to 12 wt% CaO, 8 wt% to 11 wt% MgO, 10.80 wt% to 11.68 wt% Fe_2O_3, <5 wt% Na_2O, and <5 wt% K_2O [7,8]. The basalt from Chai Badan, Lopburi contains high amount of silica; therefore, it is hardly melted and formed as basalt fiber by itself without additional fluxes.

Bottom ash from Mae Moh power plant in Lampang province, Thailand is a waste from lignite combustion. Huge amount of the bottom ash, around 0.8 million ton per year, was disposed by landfilled near the power plant [9]. A previous study has reported that the bottom ash from this source was consisted of 39.3 wt% SiO_2, 21.3 wt% Al_2O_3, 13.5 wt% Fe_2O_3, 2.1 wt% K_2O, 16.5 wt% CaO, 1.0 wt% Na_2O, and 1.4 wt% loss on ignition. It composed of both amorphous and crystalline phases which are quartz, anorthite, augite, magnetite, and hematite [9]. From the composition it showed high amount of alumina but lower silica and calcium oxide content than basalt. It is possible to mix between basalt rock from Chi Badan and the bottom ash in suitable ratio according to basalt fiber formula.

The studies on glass fiber reinforced cement (GFRC) reported the degradation of glass fiber in the cement matrix. The hydration and setting of cement process produced the portlandite ($Ca(OH)_2$) which is the cause of corrosion of the fiber [10,11]. Glass fiber in alkaline environment is rapidly deteriorate in strength, weight and diameter [12]. This process can be attributed to breaking of the Si−O−Si network in the silicate glass, by the hydroxyl ions (OH⁻) which are highly concentrated in the alkaline pore. Basalt fiber is increasingly applied in glass fiber reinforce concrete along with Alkali Resistance (AR) glass fiber. The basalt fiber is not only low price and cheaper than AR-glass fiber, but also high mechanical properties and good resistance to alkaline attack [13,14]. However, its alkali resistance is lower than of AR-glass fibers. There are many studies proposed to increase alkali resistance of glass fibers are improve glass composition [15], applying new sizing and coating [16,17], and using cement and concrete additives[18,19]. However, zirconia addition is reliable and most widely used [20-23]. The alkali resistance of glass fiber can be improved by the formation of a thin stable hydrated zirconium-rich layer on glass surface. It was formed at the first stage of alkaline attack on the silica glass network at the surface which could diminish the diffusion of OH⁻ ion into the glass [24].

In this work, basalt rock from Chai Badan with high silica content and the lignite bottom ash from Mae Moh power plant were used as a major raw material to fabricate the fiber glass in range of basalt fiber formula. The zirconia was used as ZrO_2 source in the glass formula to improve the alkali resistance of the fiber glass.

2. Experimental

2.1 Materials and glass fiber preparation

The main raw materials used to prepare a fiber sample were basalt rock collected from basalt-mining area in Chai Badan, Lopburi, Thailand (Mine Chem Co., Ltd) and the lignite bottom ash from Mae Moh powerplant, Lampang, Thailand. Their chemical compositions were obtained by X-ray fluorescence (Rigaku ZSX Primus III+, Japan) and showed in Table 1. $MgCO_3$ (> 40% MgO, Ajax Finechem) was added to balance the chemical composition of glass according to the typical composition of basalt fiber. The starting batch (BG01) was a mixture of 57.91 wt% of basalt rock, 31.43 wt% of bottom ash, and 10.66 wt% of $MgCO_3$. The glass formulas were varied the percentage of ZrO_2 content by up to 10 wt% as shown in Table 2. The mixture of raw materials was melted in an alumina crucible at 1500°C for 3 h then poured into a graphite mold. A fiber sample was prepared by rapid drawing from the molten glass.

2.2 Characterizations and properties measurements

The glass samples were prepared by melting and quenching process before ground and sieved through a 100-mesh screen. Their glassy phase and residual undissolved phase were investigated by X-ray diffraction technique, (XRD D8 ADVANCE, Germany). The XRD patterns were obtained over the 2θ range of 10° to 70°

at a scan step 2θ = 0.01°, a scan rate of 2° (2θ·min⁻¹) and operated at 40 kV and 30 mA.

The glass transition temperature (T_g), crystallization onset temperature (T_c), crystallization peak (T_p), and endothermic peak of liquidus temperature ($T_{L\ peak}$) of glass powder samples were determined by using TG-DSC (STA PT 1600, Linseis, Germany) in the temperature range from 25°C to 1200°C with heating rate of 10°C·min⁻¹.

Thin fiber samples with diameter from 50 μm to 100 μm were selected for measuring its tensile strength and alkali resistance. To measure the tensile strength of glass fiber, a glass fiber sample was prepared as shown in Figure 1. The tensile strength of a fiber sample was carried out in a UTM (universal testing machine, Instron 5843) with 45 kN capacity, and the loading rate was 5 mm·min⁻¹.

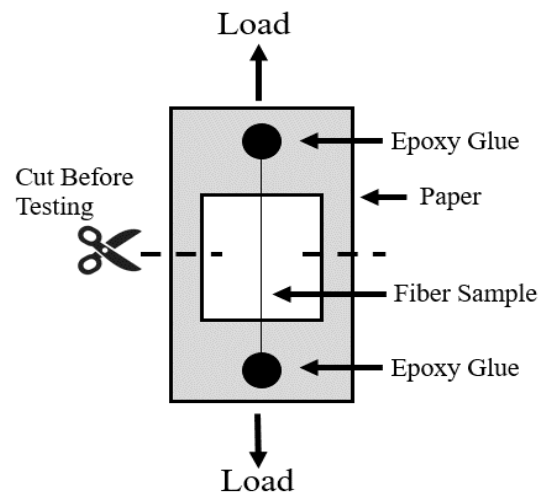**Figure 1.** Sample setup for tensile strength measurement.

Table 1. Chemical composition of basalt and bottom ash in wt%.

Oxides	SiO_2	CaO	Al_2O_3	MgO	TiO_2	Na_2O	SO_3	K_2O	MnO	Fe_2O_3	V_2O_5	Cr_2O_3	ZrO_2
Basalt rock	59.77	5.82	16.45	3.21	0.94	2.62	-	2.2	0.17	8.04	0.02	0.03	0.05
Bottom ash	30.19	25.02	14.82	2.67	0.58	0.67	2.54	2.39	0.17	19.8	0.03	0.07	0.03

Table 2. Glass formulas in wt%.

Oxides	Compositions (wt%)				
	BG01	BG02	BG03	BG04	BG05
SiO_2	46.72	45.57	44.40	43.24	42.07
Al_2O_3	15.03	14.66	14.28	13.91	13.53
Fe_2O_3	11.52	11.24	10.95	10.67	10.38
CaO	11.90	11.61	11.31	11.01	10.72
MgO	8.26	8.06	7.85	7.64	7.44
Na_2O	1.83	1.79	1.74	1.69	1.65
TiO_2	0.77	0.75	0.73	0.71	0.69
K_2O	2.15	2.09	2.04	1.99	1.93
SO_3	0.85	0.82	0.80	0.78	0.76
MnO	0.16	0.16	0.15	0.15	0.14
V_2O_5	0.02	0.02	0.02	0.02	0.02
Cr_2O_3	0.04	0.04	0.04	0.04	0.04
P_2O_5	0.11	0.11	0.10	0.10	0.10
ZrO_2	0.04	2.50	5.00	7.50	10.00

Alkali resistance of glass fibers was measured as well as the literature [22]. The accelerated aging test was achieved by refluxing them in a plastic flask with 250 mL mixture of 1 M NaOH and 0.5 M Na_2CO_3 in the ratio of 1:1. The plastic flask was put in a water bath at 98°C for 3 h. Then the fiber glass samples were rinsed with distilled water and dried. Alkali resistance of the glass fibers was determined by the weight loss after treatment.

Visual observation of the fiber samples was observed by optical microscope (Olympus BX51 TRF). The microstructure of corrosion and crystallization deposited on the alkali treatment fiber were studied by Scanning electron microscopy (SEM, JEOL JSM-6610LV) and energy dispersive X-ray spectroscopy (EDS, Oxford X-MaxN 50 EDS).

3. Results and discussion

3.1 As melted glass and fiber form basalt and lignite bottom ash

Basalt rock in this study has high concentration of SiO_2 and Al_2O_3, therefore, it cannot be melted at 1500°C without fluxing agents. The mixture of glass batch with addition of lignite bottom ash played a role in reducing the melting temperature by increasing of CaO content in basaltic glass composition. The starting glass batch containing basalt and lignite bottom ash, BG01 was completely melted at 1500°C with soaking time of 3 h. From the chemical composition analysis result, there was 2.54 wt% of SO_2 in bottom ash. According to a previous study, some crystalline phases of anhydrite ($CaSO_4$) and gypsum ($CaSO_4\cdot2H_2O$) were detected in the bottom ash from Mae Moh power plant [25]. Anhydrite can be formed by dehydration process upon heating. After dehydration of gypsum, anhydrite is decomposed at 900°C to form SO_2 [26]. This resulted in the formation of bubble between heating in the crucible on melting process, however, the bubbles were completely released after soaking at elevated temperature. As quenched glass samples were dark brown to black glass without bubble and undissolved phase, from visual inspection. The glass batches with varying the ZrO_2 content from 2.5 wt% to 7.5 wt% ZrO_2 (BG02, BG03, BG04) were also completely melted without undissolved phase. There were some crystalline phases found at the bottom and wall of the crucible after poured the melt of the batch containing 10 wt% ZrO_2 (BG05). The XRD-patterns of all glass samples are amorphous as shown in Figure 2 however, it was found the crystalline phase in the bottom of the crucible of BG05 glass formula. The sample labeled BG05X in Figure 2 is the XRD-pattern of glass containing small pieces of zirconia crystal in the bottom of BG05 crucible. The BG05 is the glass containing 10 wt% ZrO_2. The crystallization was occurred in the bottom of crucible in consequence of the solubility limit of ZrO_2 in basalt glasses which was determined to be 7.1 wt% to 7.5 wt% according to the literature [20] and the previous work [27] respectively. A continuous glass fiber sample with diameter less than 100 μm were obtained from all glass formulas.

3.2 Thermal properties

The as-quenched glasses were characterized by DTA. The DTA traces of all sample are shown in Figure 3. Those traces show the same characteristic patterns which can be determined the glass transition

temperature (T_g), the onset of crystallization temperature (T_c), the crystallization peak temperature of the first crystalline phase (T_{p1}), the crystallization peak temperature of the second crystalline phase (T_{p2}), and the end point of endothermic peak associated with endothermic peak of liquidus temperature ($T_{L\ peak}$). Table 3 shows the characteristic temperature of the glass samples. The T_g of glass seems increase with increasing of ZrO_2 content in glass samples. The T_g of glass is corelated with viscosity. This result shows the increase amount of ZrO_2 affected in increase the viscosity of glass. The greater viscosity in the glass also retards the crystallization upon heating, by which it means that the glass needs higher temperature to reduce its viscosity then the crystallization can occur. It was found that the sample with greater content of ZrO_2, therefor, has greater crystallization temperature. The endothermic peaks of liquidus temperature were found in the DTA curve of BG02 - BG05 samples, however, they are quite the same temperature.
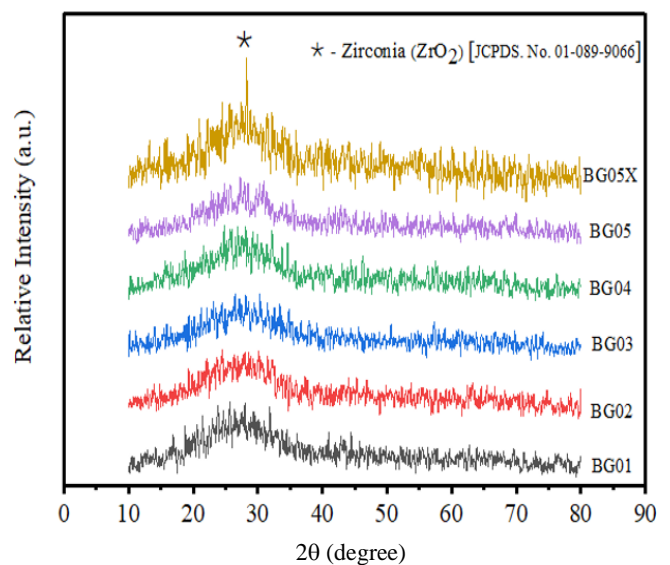

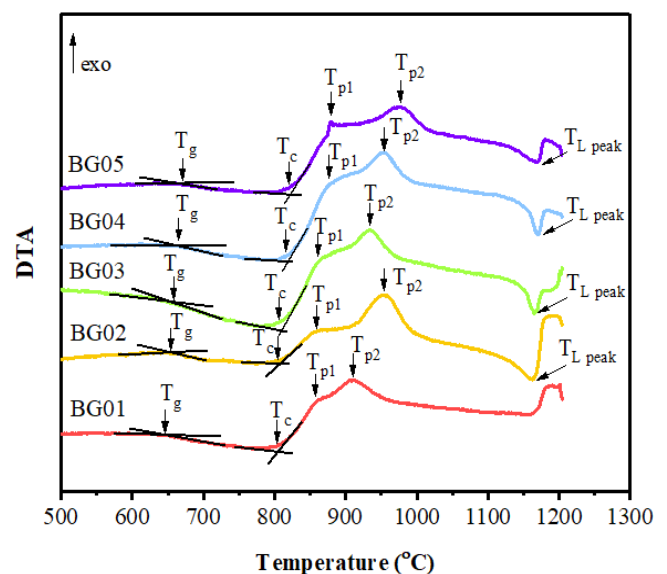**Figure 2.** XRD-patterns of as-melted glass samples.

**Figure 3.** DTA curves of as-melted glass samples.

Table 3. Thermal properties of as-melted glass (in °C).

| Sample	T_g	T_c	T_{p1}	T_{p2}	$T_{L\ peak}$
BG01	645.59	804.68	860.20	903.27	-
BG02	652.86	805.09	862.32	954.33	1163.03
BG03	656.94	809.83	863.32	933.14	1166.11
BG04	665.57	818.61	875.94	951.91	1169.03
BG05	671.85	821.93	880.78	973.40	1168.85

3.3 Mechanical properties

The comparison of tensile strength of glass fiber samples is shown in Figure 4 and the other mechanical properties are shown in Table 4. Among the glass fiber samples, BG03 with 5 wt% ZrO_2 content has the highest ultimate tensile strength. The average ultimate tensile strength of BG03 and BG04 are 796±141 and 774±71 MPa respectively. It is noticed that the difference of these values is not significant because of a large standard deviation. The correlation between ZrO_2 content in a fiber sample and the ultimate tensile strength is that the increase of ZrO_2 from 0 wt% to 5 wt% in glass formula encouraged the strength of the glass fiber. This result showed that increasing content of ZrO_2 improved the strengths by the ZrO_2/SiO_2 substitution strengthens the silicate network as well as the study of the properties of silicate glass containing zirconia reported by R. Karell *et al.* [28]. ZrO_2 in this study possible to be 6-coordination zirconium in silicate glass as well as alumina or it call "network modifier". It not only takes part in the formation of the silicate network but in addition it heals the broken Si-O-Si bridges (eliminate non-bridging oxygen). The increasing of T_g with increasing ZrO_2 content in glass sample also proves the strengthening of silica network in this work. The strength of glass decreased dramatically in case of 10 wt% ZrO_2 containing glass, BG05. From optical observation in Figure 5, the crystalline phases found as a defect at fracture origin of BG05 fiber sample after tensile testing, while there is no defect found in the other samples. The pictures of fracture origin without defect of BG03 and BG04 fiber are also shown in Figure 5. The small number of crystalline phases could not be detected in XRD intensity. The crystalline phase found in BG05 fiber containing 10 wt% of ZrO_2,

was the crystallization of ZrO_2 by the solubility limit of ZrO_2 in basalt glasses. The thermal expansion mismatch between crystalline and glassy phase is the cause of the thermal stress surrounding the crystal in a glass fiber. It was occurred during the fiber forming process with a rapid cooling rate. The crystals in the melt may be drawn from the crucible with a fiber. The stress concentration at defect tips can initiate crack propagation after applying an external load. In case of greater concentration of ZrO_2 in silicate glass, the Zr^{4+} also acts as a modifier increase the non-bridging oxygen in the glass network when a certain threshold is reached, zirconium surplus leads to break a glass structure and a reduction of the tensile strength [22].
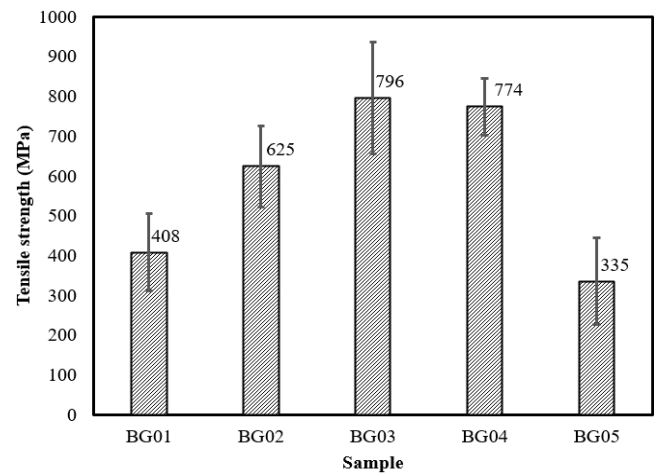
Figure 4. Tensile strength of a single fiber sample.

Table 4. Mechanical properties of glass samples from single-fiber test results.

Sample	Tensile strength (MPa)	Elongation at break (%)	Modulus of elasticity (GPa)
BG01	408±98	0.72±0.12	56.4±7.6
BG02	625±102	0.81±0.14	78.2±11.8
BG03	796±141	0.96±0.22	83.6±11.2
BG04	774±71	1.05±0.20	75.7±14.6
BG05	335±109	0.88±0.03	37.6±11.4
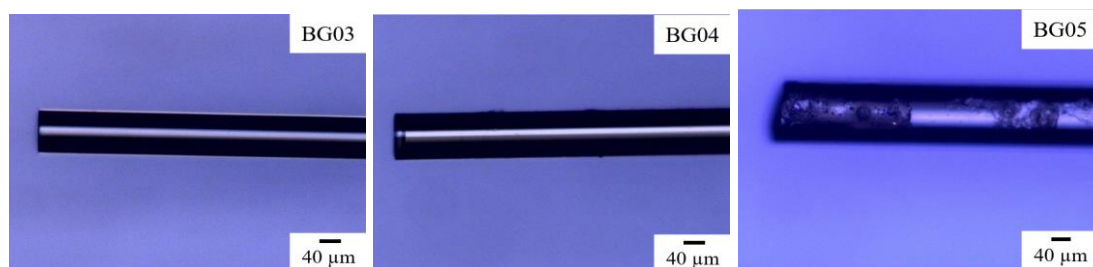
Figure 5. Optical microscopy image of fractured fibers.

3.4 Alkali resistivity

From the accelerated aging test, the percentage of weight loss by alkali attack of each sample is plotted in Figure 6. At low concentration of ZrO$_2$, the results have shown a greater weight loss of 26.45% and 23.33% found in a glass fiber containing 0% ZrO$_2$, BG01 and 2.5% ZrO$_2$, BG02 respectively. The corrosion rate of glass fiber with ZrO$_2$ content from 5 wt% to 10 wt% decreased slightly with increasing of ZrO$_2$ content. It decreased from 7.51% to 4.32%. BG04 performed the best alkali resistance from this result. The corrosion in alkali solution was the result from breaking of silica glass network by hydroxyl ion and the aluminosilicate phases, found on the surface of all samples. From EDS analysis, there are two types of crystalline phases precipitated as a shell on the surface of basalt fibers.

The first one was CaCO$_3$ which crystallized both cubic and rod-like shape as marked at point 1 and 4 in Figure 8. The CaCO$_3$ crystals were crystallized due to diffusion of Ca ion in the glass fiber to the surface and penetration of CO$_2$ in the bottle into the alkali solution during alkali resistance testing process. The plate-like hexagonal crystals (Figure 8. Point 2 and 3) was started from iron hydroxide carbonate Fe$_6$(OH)$_{12}$CO$_3$ which oriented perpendicular to the surface of the fiber [29]. The corrosion shell was delaminated by increasing of its thickness, the corrosion of fresh surface, then continued. There was found that the thin layer of crystal shells remains on the surface of BG04 and BG05 after rinsed much higher than the lower ZrO$_2$ containing fiber (see Figure 7). This can be explained that the corrosion shell thickness of higher ZrO$_2$ content fiber increases at slower rate according to its higher alkali resistance. The thicker shell can be detached easily, while the thin layer of corrosion shell remains on the surface. It acts as a protection layer at the beginning of corrosion process by slowing down the attack of alkali on the fresh surface of glass fiber.
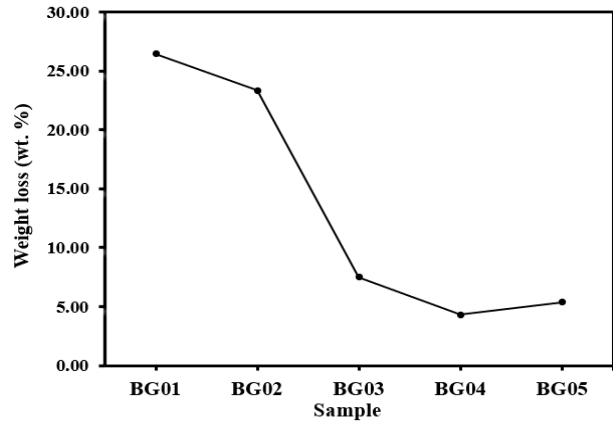
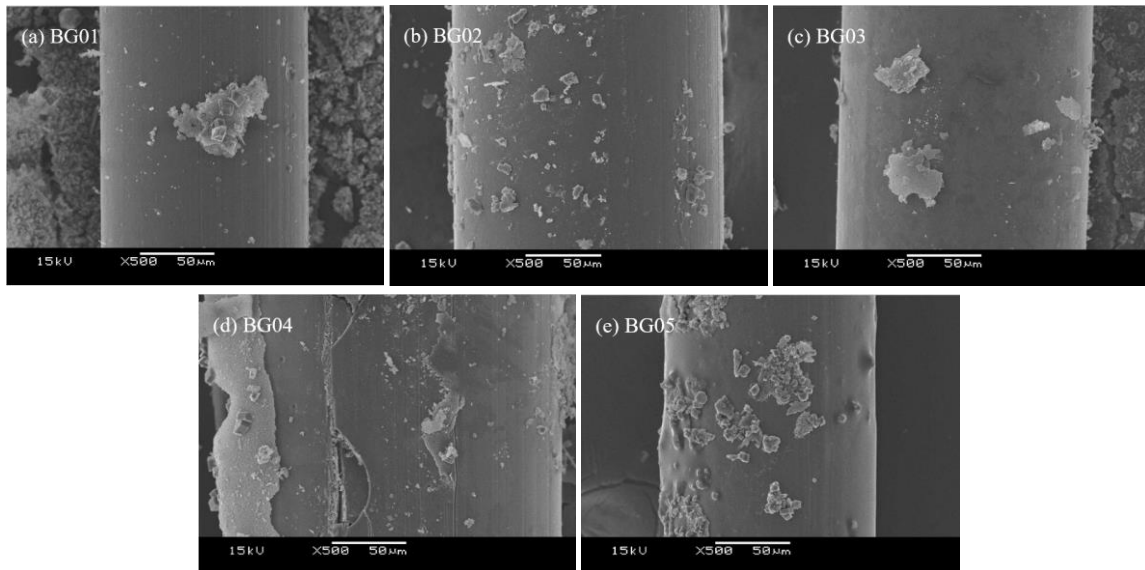**Figure 6.** Weight loss of the glass fiber samples after alkali immersion.

Figure 7. SEM image of the glass fiber samples after alkali immersion.

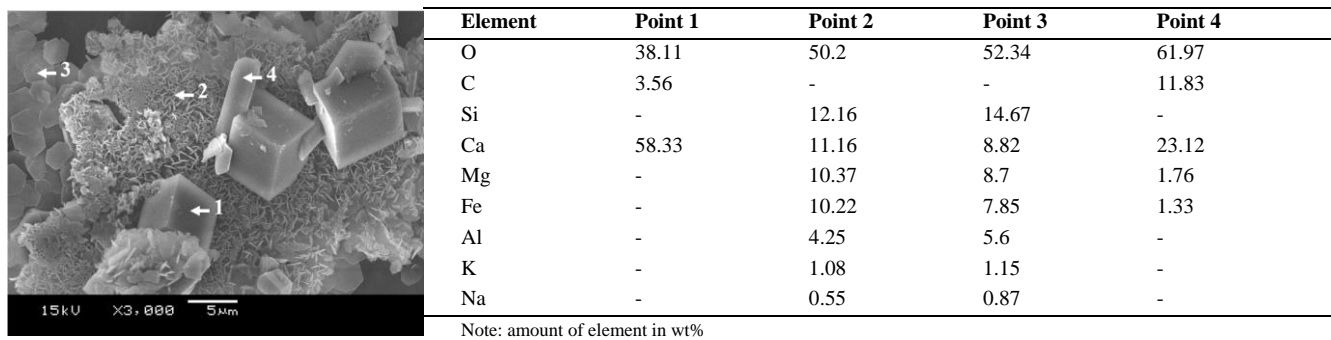| Element	Point 1	Point 2	Point 3	Point 4
O	38.11	50.2	52.34	61.97
C	3.56	-	-	11.83
Si	-	12.16	14.67	-
Ca	58.33	11.16	8.82	23.12
Mg	-	10.37	8.7	1.76
Fe	-	10.22	7.85	1.33
Al	-	4.25	5.6	-
K	-	1.08	1.15	-
Na	-	0.55	0.87	-
Note: amount of element in wt%				

Figure 8. SEM image and results of EDS analyses taken from indicated points.

4. Conclusions

The glass fiber according to basalt fiber composition were successful prepared from the mixture of silica rich basalt rock from Chai Badan, Lopburi, Thailand and lignite bottom ash, from Mae Moh power plant. The addition of 0-10 wt% of ZrO_2 in glass formula resulted in increase its viscosity by shifting the glass transition temperature and crystallization temperature to higher value. The addition of ZrO_2 content in glass fiber composition also increase the alkali resistivity and improving tensile strength of the fiber through strengthening the glass network the ZrO_2/SiO_2 substitution strengthens. The glass fiber formula with 7.5 wt% of ZrO_2 content performed the highest alkali resistance and tensile strength. The addition of ZrO_2 in the glass fiber should not be more than 7.5 wt% because of the solubility limit of ZrO_2.

References

[1] H. Jamshaid, "Basalt fiber and its applications," *Journal of Textile Engineering & Fashion Technology,* vol. 1(6), pp. 254-255, 2017.

[2] J. Militký, V. R. Kovačič, and J. Rubnerová, "Influence of thermal treatment on tensile failure of basalt fibers," *Engineering Fracture Mechanics,* vol. 69(9), pp. 1025-1033, 2002.

[3] V. Fiore, T. Scalici, G. Di Bella, and A. Valenza, "A review on basalt fibre and its composites," *Composites Part B: Engineering,* vol. 74, pp. 74-94, 2015.

[4] S. M. Barr, and A. S. MacDonald, "Geochemistry and geo-chronology of late cenozoic basalts of southeast Asia," *Bulletin of the Geological Society of America,* Article vol. 92, no. 8 PART2, pp. 1069-1142, 1981.

[5] S. Intasopa, T. Dunn, and R. S. Lambert, "Geochemistry of Cenozoic basaltic and silicic magmas in the central portion of the Loei–Phetchabun volcanic belt, Lop Buri, Thailand," *Canadian Journal of Earth Sciences,* vol. 32(4), pp. 393-409, 1995.

[6] V. Dhand, G. Mittal, K. Y. Rhee, S. -J. Park, and D. Hui, "A short review on basalt fiber reinforced polymer composites," *Composites Part B: Engineering,* vol. 73, pp. 166-180, 2015.

[7] J. Militký, V. Kovačič, and J. Rubnerová, "Influence of thermal treatment on tensile failure of basalt fibers," *Engineering Fracture Mechanics,* Article vol. 69(9), pp. 1025-1033, 2002.

[8] T. Deák, and T. Czigány, "Chemical Composition and Mechanical Properties of Basalt and Glass Fibers: A Comparison," *Textile Research Journal,* Article vol. 79(7), pp. 645-651, 2009.

[9] A. Sathonsaowaphak, P. Chindaprasirt, and K. Pimraksa, "Workability and strength of lignite bottom ash geopolymer mortar," *Journal of Hazardous Materials,* vol. 168(1), pp. 44-50, 2009.

[10] N. Arabi, L. Molez, and D. Rangeard, "Durability of alkali-resistant glass fibers reinforced cement composite: Microstructural observations of degradation," *Periodica Polytechnica Civil Engineering,* Article vol. 62(3), 2018.

[11] A. Bentur, and S. Mindess, *Fiber Reinforced Cementitious Composites*, second edition ed. London and New York: Taylor and Francis, 1990.

[12] R. J. Charles, "Static Fatigue of Glass. I," *Journal of Applied Physics,* vol. 29(11), pp. 1549-1553, 1958.

[13] S. I. Gutnikov, A. P. Malakho, B. I. Lazoryak, and V. S. Loginov, "Influence of alumina on the properties of continuous basalt fibers," *Russian Journal of Inorganic Chemistry,* Article vol. 54(2), pp. 191-196, 2009.

[14] B. E. Ramachandran, V. Velpari, and N. Balasubramanian, "Chemical durability studies on basalt fibres," *Journal of Materials Science,* Article vol. 16(12), pp. 3393-3397, 1981.

[15] A. J. Majumdar, J. M. West, and L. J. Larner, "Properties of glass fibres in cement environment," *Journal of Materials Science,* Article vol. 12(5), pp. 927-936, 1977.

[16] V. A. Rybin, A. V. Utkin, and N. I. Baklanova, "Alkali resistance, microstructural and mechanical performance of zirconia-coated basalt fibers," *Cement and Concrete Research,* Article vol. 53, pp. 1-8, 2013.

[17] S. L. Gao, E. Mäder, and R. Plonka, "Coatings for glass fibers in a cementitious matrix," *Acta Materialia,* Article vol. 52(16), pp. 4745-4755, 2004.

[18] A. Nourredine, "Influence of curing conditions on durability of alkali-resistant glass fibres in cement matrix," *Bulletin of Materials Science,* Article vol. 34(4), pp. 775-783, 2011.

[19] M. Butler, V. Mechtcherine, and S. Hempel, "Durability of textile reinforced concrete made with AR glass fibre: Effect of the matrix composition," *Materials and Structures/ Materiaux et Constructions,* Article vol. 43(10), pp. 1351-1368, 2010.

[20] Y. V. Lipatov, S. I. Gutnikov, M. S. Manylov, and B. I. Lazoryak, "Effect of ZrO_2 on the alkali resistance and mechanical properties of basalt fibers," *Inorganic Materials,* Article vol. 48(7), pp. 751-756, 2012.

[21] M. Kukizaki, "Large-scale production of alkali-resistant Shirasu porous glass (SPG) membranes: Influence of ZrO_2 addition on crystallization and phase separation in Na_2O-CaO-Al_2O_3-B_2O_3-SiO_2 glasses; and alkali durability and pore morphology of the membranes," *Journal of Membrane Science,* Article vol. 360(1-2), pp. 426-435, 2010.

[22] Y. V. Lipatov, S. I. Gutnikov, M. S. Manylov, E .S. Zhukovskaya, and B. I. Lazoryak, "High alkali-resistant basalt fiber for reinforcing concrete," *Materials & Design,* vol. 73, pp. 60-66, 2015.

[23] K. Kamiya, S. Sakka, and Y. Tatemichi, "Preparation of glass fibres of the ZrO_2-SiO_2 and Na_2O-ZrO_2-SiO_2 systems from metal alkoxides and their resistance to alkaline solution," *Journal of Materials Science,* Article vol. 15(7), pp. 1765-1771, 1980.

[24] M. Butler, V. Mechtcherine, and S. Hempel, "Experimental investigations on the durability of fibre-matrix interfaces in textile-reinforced concrete," *Cement and Concrete Composites,* Article vol. 31(4), pp. 221-231, 2009.

[25] A. Rungchet, C. S. Poon, P. Chindaprasirt, and K. Pimraksa, "Synthesis of low-temperature calcium sulfoaluminate-belite cements from industrial wastes and their hydration: Comparative studies between lignite fly ash and bottom ash," *Cement and Concrete Composites,* vol. 83, pp. 10-19, 2017.

[26] S. Matsuya and M. Yamane, "Decomposition of gypsum bonded investments," (in eng), *J Dent Res,* vol. 60(8), pp. 1418-1423, 1981.

[27] N. Vaiborisut, C. Chunwises, D. Boonbundit, S. Jiemsirilers, and A. Theerapapvisetpong, "Effect of the Addition of ZrSiO$_4$ on Alkali-Resistance and Liquidus Temperature of Basaltic Glass," *Key Engineering Materials,* vol. 766, pp. 145-150, 2018.

[28] R. Karell, J. Kraxner, and M. Chromčíková, "Properties of selected zirconia containing silicate glasses," *Ceramics - Silikaty,* Article vol. 50(2), pp. 78-82, 2006. [Online]. Available: https://www.scopus.com/inward/record.uri?eid=2-s2.0-33745867238&partnerID=40&md5=5f0eec8d4bf5e202d727f5e4072bfe73.

[29] V. A. Rybin, A. V. Utkin, and N. I. Baklanova, "Corrosion of uncoated and oxide-coated basalt fibre in different alkaline media," *Corrosion Science,* vol. 102, pp. 503-509, 2016.

[30] Q. Wang, Y. Ding, and N. Randl, "Investigation on the alkali resistance of basalt fiber and its textile in different alkaline environments," *Construction and Building Materials,* vol. 272, pp. 121670, 2021.